

Generic origins of irregular spiking in neocortical networks

R. Stoop^{1,2}, L. A. Buzimovich³, W.-H. Steeb⁴

¹Institute for Neuroinformatics, UNIZH/ETHZ, Zürich, Switzerland

²Technical University of Applied Sciences Nordwestschweiz, Solothurn, Switzerland

³Georgia Institute of Technology, Atlanta, Georgia, USA

⁴Rand Afrikaans University, Johannesburg, South Africa

Received: 23 December 1998 / Accepted in revised form: 9 June 2000

Abstract. We identify generic sources of complex and irregular spiking in biological neural networks. For the network description, we operate on a mathematically exact mesoscopic approach. Starting from experimental data, we determine exact properties of noise-driven, binary neuron interaction and extrapolate from there to properties of more complex types of interaction. Our approach fills a gap between approaches that start from detailed biophysically motivated simulations but fail to make mathematically exact global predictions, and approaches that are able to make exact statements but only on levels of description that are remote from biology. As a consequence of the approach, a novel coding scheme emerges, shedding new light on local information processing in biological neural networks.

1 Noise-driven neurons

In our study, we focus on the properties of pyramidal neurons that make up about 70% of all cortical neurons. From physiological observations, these cells are expected to be of special importance for the integrative tasks in biological neural networks. The vast majority of the pyramidal neurons outside of layer V consist of intrinsically regularly spiking neurons (Abeles 1982; Koch 1999). Our approach to studying generic biological neuron interaction is based upon the distinction of different levels of synaptic input to these cells. Although synaptic transmitter release is quantal, different orders of magnitude of input are received:

1. *Small-scale input* (e.g. from remote synapses) drives the neuron towards regular spiking with well-defined spiking frequency. This small-scale input will be referred to as *noisy input*. It is able to reflect local gradients of excitation in the network.

2. *Strong input* from next neighbors (i.e. from strongly connected neurons or from groups of synchronized neurons).
3. *Medium-size interactions* that may take account of changing neighborhood conditions on time scales typically of the order of an interspike interval.

Due to the enormous number of synaptic contacts, a large number of small-scale synaptic inputs arrive at a typical neuron (Abeles 1982; Koch 1999). Assuming a Gaussian central limit behavior of this input [other distributions that allow for a well-defined average are also suitable (Feller 1971)], an almost constant inflow of charge results that can be identified with a constant driving current. This point of view is also adopted in most simulation approaches (Hines 1989, 1994). To this driving current, simple pyramidal neurons respond with regular spiking. Mathematically, this behavior is described by a *limit-cycle*. Limit cycles are objects by mathematical abstraction, like fixed-points, defined in terms of characteristic stability properties of their response to perturbations. Abstract models of pyramidal neurons fulfil these criteria. The proof that also biological pyramidal neurons are limit cycles has been given in detail in (Stoop et al. 2000a). Substantial input by strongly connected neurons or by strongly synchronized groups of neurons lead to considerable perturbations of these limit-cycles. This is our concept of *noise-driven neocortical interaction*. In our opinion, part of the complicated geometrical structure of the neuronal dendrites may only serve to establish reliable stable driving currents, where it is perfectly possible that different functional driving currents could be generated on the same neuron. This aspect of our approach is similar to the recent observation that, on the microscopic level, thermal noise can be converted into directed activity (by so-called Brownian motors (Chillemi and Barbi 1999)). In our investigation, effects generated by strong waves of neural excitability will be excluded. Under these *quasistatic* network conditions, *spike-time coded information transmission* is naturally prevalent.

2 Interaction of noise-driven neurons

The response of a regular spiking neuron upon a strong synaptic perturbation is the main biological ingredient in our approach. This characteristic of a neuron can be captured in the *phase-response function* $g(\phi)$, which measures the lengthening/shortening effect to the unperturbed interspike interval, as a function of the phase ϕ at which a strong synaptic perturbation of strength K arrives. If i denotes the perturbed and u the unperturbed interval length, we have $g(\phi) = i(\phi)/u$, which is equally easily calculated in simulations and in experiments. We start our presentation by focusing on fixed values of K , until we include the dependence on the perturbation strength in a straightforward way.

In our experiments with real neurons, slices of rat neocortex were prepared for in vitro recording. Following standard techniques, simple pyramidal neurons of the barrel cortex were intracellularly recorded with sharp electrodes. To induce regular firing, a constant current was injected into the neurons (Abeles 1982; Reyes and Fetz 1993; Koch 1999). Regularly firing neurons were periodically perturbed by strong extracellular stimulations of synaptic inputs to the neurons. Excitatory perturbations were generated by the stimulation of adjacent white or gray matter by means of bipolar electrodes. Inhibitory perturbations were generated when fast excitatory transmission was pharmacologically blocked by application of DNQX and AP5, while regular current pulses were applied to fibers making a synaptic contact with the regularly firing neuron. Typical results of our experiments are shown in Fig. 1, for inhibitory and for excitatory perturbations. In the context of in vivo neural networks, these perturbation paradigms can be regarded as the representations of synaptic inputs from strong synaptic connections (Reyes and Fetz 1993). Our approach can be seen as an extension of related experiments described in detail by Reyes and Fetz. Our related theoretical development, however, leads in entirely new directions.

In our study, we are interested in the properties of networks of simple pyramidal neurons, into which both excitatory and inhibitory connections are incorporated. A simple case of such networks can be built up from intrinsically regularly firing neurons that are under continued perturbations by other neurons. Since the effects of perturbations decrease as a function of the topological neighboring order, in our model the perturbations are restricted to emerge from a number m of next-neighbors, where we define as next-neighbors those neurons from which the strongest perturbations result. For all presented simulations, we choose the checkerboard ($m = 4$) topology of interaction, and the distribution between inhibitory and excitatory connections always reflects the generic situation in the neocortex (1 inhibitory: 4 excitatory connections). To represent the variability seen in biological networks, the remaining interaction characteristics (perturbation strengths K , spiking frequencies, interaction types) are chosen at random, and then, unless stated otherwise, held fixed. With the help of the experimentally measured pertur-

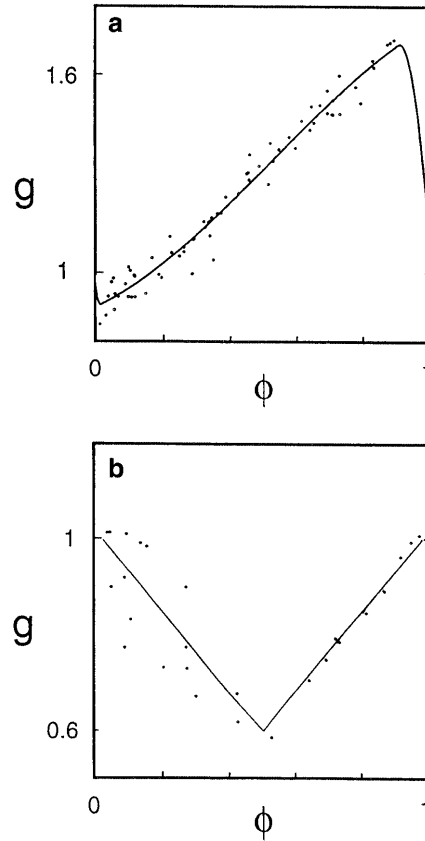


Fig. 1. Experimental measurements (*dots*) of the relative change of the interspike interval length, for perturbations of fixed strength K applied at variable phases ϕ , together with the interpolating phase response function $g(\phi)$, for (a) inhibitory, and (b) excitatory interaction. For some experimental cells, the refractory period cannot be neglected. The functional description of the inhibitory map is approximately

$$\begin{aligned}
 g(\phi)_{\text{inh}} &= 0.611432 + 5.37780\phi + 0.00777/(0.02 + \phi) && \text{for } 0 < \phi \leq 0.02; \\
 &= 0.90326 + 0.48012\phi + 1.03433\phi^2 - 0.65917\phi^3 && \text{for } 0.02 < \phi \leq 0.9; \\
 &= 394.32344 - 144.92539\phi - 471.95630/(0.9 + \phi) && \text{for } 0.9 < \phi \leq 1.
 \end{aligned}$$

In addition to the presented piecewise linear excitatory map $g(\phi)_{\text{exc}}$, we also used variants with (horizontal) refractory period extending to $\phi = 0.15$ and cosine-modeled descending part for $0.15 < \phi \leq 0.3$

bation response functions $g(\phi)$ (cf. Fig. 1), the described concept can be implemented in a straightforward way. In Fig. 2, the described network topology, the principles of the interaction, and a typical result are shown.

Figure 2 shows, for one typical neuron, the resulting spiking behavior. In the figure, the deviation at the n th spike event between average-based expected and actual spike time, $\text{dev}(n) := n \delta t_{\text{av}} - \sum_i^n \delta t_i$, is displayed (where δt_i denotes i th and δt_{av} denotes the over a sufficiently long time averaged mean interspike interval. For the plot, linear interpolation between spiking events has been used). The complexity of the spiking behavior is obvious, in spite of the simplicity of the network. Along

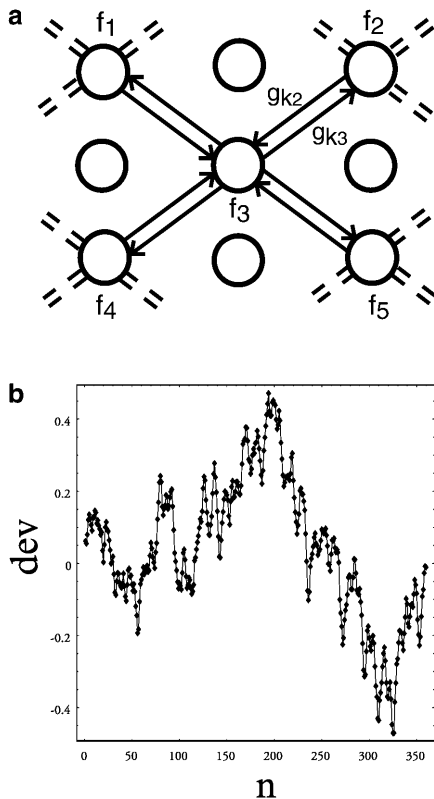


Fig. 2. **a** Topology of the simplest type of network of intrinsically regularly spiking, via $g(\phi)$ interacting, neurons. Each neuron is perturbed by four next-neighbors, providing inhibitory/excitatory synaptic input. A neuron's spiking time is determined by its intrinsic interspike interval plus the effects of past perturbations. The effect of a perturbation depends on the strength of the connection, the excitability of the target neuron (both contained in K), and on the phase of its arrival. **b** Complex behavior emerging from this network, demonstrated by the deviation dev between expected and actual spike time, measured for a particular neuron (see text)

with obviously non-periodic behavior, locally induced low-order periodicity is often found to modulate globally induced irregular spiking behavior.

A rather precise idea of the origin of this complexity can be obtained from binary interaction alone. Binary interactions are characterized by various bifurcation cascades that emerge both as a function of the involved firing frequencies and of the interaction strength K (Stoop et al. 1999). To arrive at a more detailed description of these phenomena, it is useful to focus on the phases at which the perturbations arrive, defined with respect to the neuron's unperturbed spiking. In a standard way, the temporal succession of phases is captured by the *phase-return function* f_Ω (Glass et al. 1984; Glass and Mackey 1988) that, mathematically, has the form of a *circle map* (Cornfeld et al. 1982):

$$f_\Omega: \phi_2 := \phi_1 + \Omega - g(\phi_1), \text{ mod } 1, \quad (1)$$

where the parameter Ω is the ratio of the intrinsic interspike time T_s of the targeting neuron divided by the interspike time T_o of the targeted neuron (Glass et al. 1984; Glass and Mackey 1988); ϕ_2 is the phase of the next perturbation, if the last perturbation arrived at

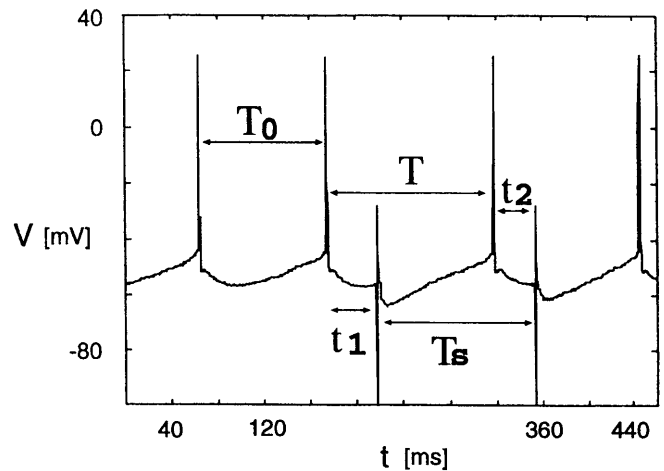


Fig. 3. Example of an experimental spike train, where the characteristic quantities T_o , T , t_1 , t_2 , and T_s are indicated. From this, the evaluation of the function g and the derivation of (1) are immediate

phase ϕ_1 . Relation (1) can immediately be derived from Fig. 3. The same figure also illustrates how function g , which is most essential to (1), can be determined from measurements. Iteration of f_Ω describes the effect of a continued regular perturbation of the neuron, where the generated sets of phases unambiguously characterize the associated firing patterns. From the observed phases, the extraction of the periodicity (if the emergent spiking is periodic) as well as the distinction of differently ordered orbits of the same periodicity, is straightforward (Let ϕ_i denote the phases at which the i th perturbation arrives. The periodicity of the spiking then is defined as the positive integer $p := \text{Min}\{q/\phi_i = \phi_{i+q}, \text{ for all } i\}$).

On the basis of extensive experiments, we were able to include the dependence on the stimulation strength K . Define first the reference curve g_{K_o} as the g -function that is measured at 75% of the maximal experimentally applicable perturbation strength. The experimental observation is that the effect of a perturbation is, to high accuracy, a linear function of K , at all phases of the interspike interval and for both stimulation paradigms.

As a consequence, we obtain a stimulation strength-dependent response function $g_K(\phi)$ of the form (Stoop et al. 2000b)

$$g_K(\phi) := (g_{K_o}(\phi) - 1)K + 1. \quad (2)$$

Numerical simulations with the corresponding phase-return function

$$f_{\Omega K}: \phi_{i+1} := \phi_i + \Omega - g_K(\phi_i), \text{ mod } 1, \quad (3)$$

show that the perturbed spiking behavior is governed by the phenomenon of locking to periodic behavior, an effect that is generically observed for interacting oscillators (Cornfeld et al. 1982). Figure 4 illustrates this principle for fixed $K = 1$, where locking is characterized by the step-wise dependence of the observed periodicity p as a function of Ω .

Locking also emerges as a function of the parameter K . A well-established mathematical fact assures that for

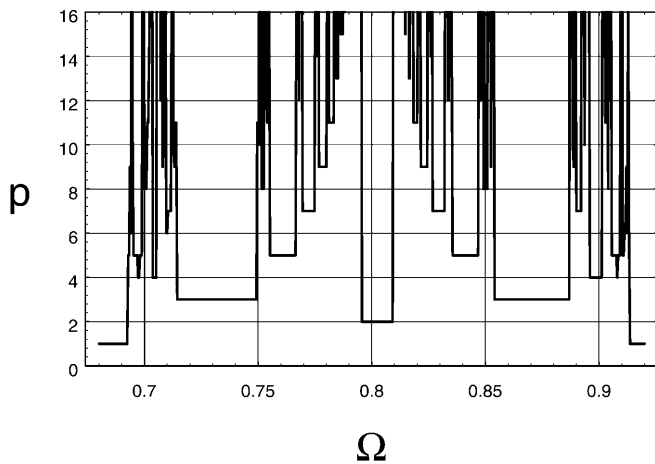


Fig. 4. Locking of the firing patterns to periodic response of periodicity p , as a function of variable Ω , but at fixed $K = 1$. The sequence of periodicities p can be interpreted as encoding of the corresponding trajectory in the $\{\Omega, K\}$ -parameter space (see Sect. 3)

every (in our experiment) accessible value of K , upon variation of Ω all positive integer periodicities p appear (Cornfield et al. 1982; Glass et al. 1984; Glass and Mackey 1988; Stoop et al. 2000b), but with ever-smaller support in the $\{\Omega, K\}$ -parameter space.

As an extension of previous work (Schindler et al. 1997) by refined *synaptic* stimulation techniques, we compared $f_{\Omega K}$ -predicted spiking properties of perturbed neurons with slice experiments of continued excitatory and inhibitory perturbations, and with sweepings of continued perturbations over ranges of Ω . In these experiments, excellent agreement between prediction and experiment was obtained. For a comparison between

predictions and experiments, the stability properties of the predicted spiking patterns, as a function of $\{\Omega, K\}$, are of importance. The stability of orbits is commonly measured in terms of *Lyapunov exponents* $\lambda_{\{\Omega, K\}}$, which measure the exponential separation rates to neighboring orbits in the tangent bundle (Peinke et al. 1992). In Fig. 5, the Lyapunov exponents are calculated over the $\{\Omega, K\}$ -parameter space, for the inhibitory perturbation paradigm.

Characteristic in this figure are the deep scars in the emergent triangular sheet at height zero. These structures, called *Arnol'd tongues*, indicate strong stability properties of the associated spiking patterns [$\lambda_{\{\Omega, K\}} < 0$ (Peinke et al. 1992)]. Each tongue comprises only one specific periodicity p . However, for each periodicity there are tongues for every possible ordering of the orbit (as is indicated in Fig. 4; see also Stoop et al. 1999). Zooming in on this figure reveals that for inhibition, *chaotic behavior* is possible in the boxed $\{\Omega, K\}$ -region [$\lambda_{\{\Omega, K\}} > 0$ (Peinke et al. 1992), at least from the numerical point of view]. However, large input strengths are needed to generate this response. Analytical investigations corroborate this observation. It is possible to prove that chaotic behavior indeed occurs on an open set of *positive Lebesgue measure* in the parameter space (Stoop et al. 2000b); to obtain more insight into the problem and into the involved technicalities, the reader may also consult Stoop and Steeb (1997). As a consequence, chaos should be experimentally observable, or the system could be tuned to chaotic states. These exact results are obtained for binary interaction; however, they also extend to higher n -ary interaction ($n = 3, 4, \dots$), for which similar results are obtained (Baesens et al. 1991). As a consequence, the following

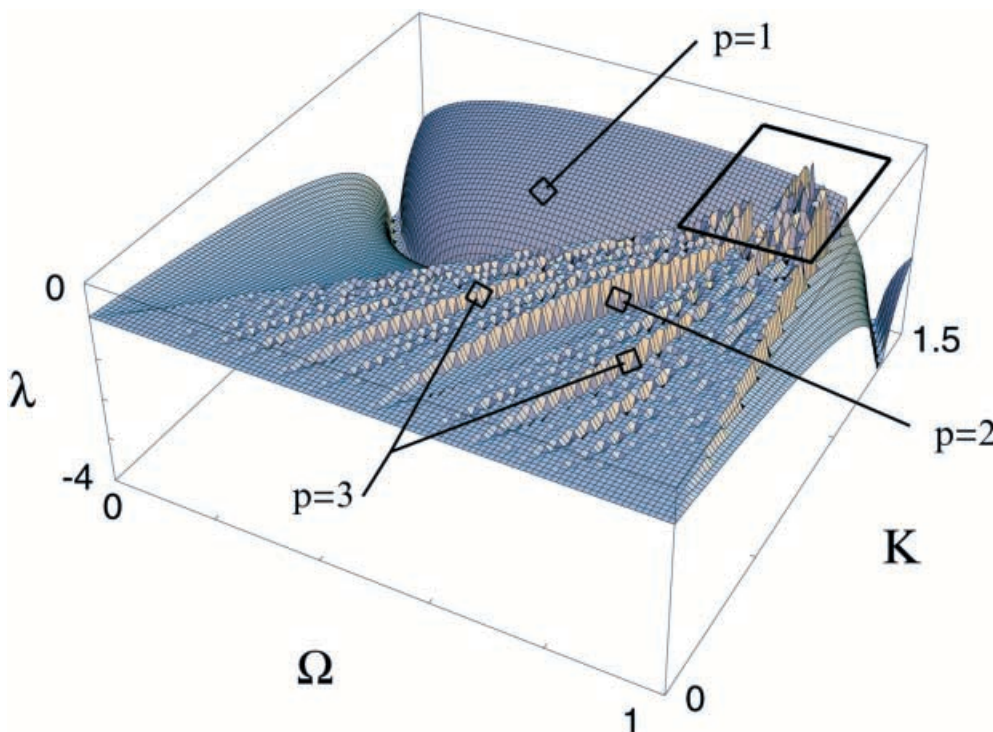


Fig. 5. Lyapunov exponents λ express the stability of the inhibitory binary neuron interaction as a function of the natural parameter space. $\lambda > 0$ indicates unstable, $\lambda < 0$ indicates stable response. Observe the emergence of the scars in the plot, the so-called *Arnol'd tongues*. On each scar, the periodicity p of the perturbed neuron's response is fixed, as is indicated for the lowest periodicities. In general, the lower the periodicity p , the more stable the neuron's response. The box indicates the location where chaotic response occurs. Similar results are obtained for excitation, which, however, fails to reach the region associated with chaotic behavior (the biological cell is unable to endure excitatory inputs of the required strength)

spiking behavior of noise-driven neocortical networks emerges:

1. Locally, low-periodic spiking behavior may be expected in abundance, by the interaction of otherwise freely spiking neurons. This periodic response is organized along Arnol'd tongues and obeys the circle-map class universality (Argyris et al. 1994).
2. As a consequence, the network is able to respond locally with any desired periodicity. While for weak local interaction the local spiking behavior is dominated by a wealth of different periodicities, for stronger interaction there is a tendency for the response to settle towards simpler, and more stable, spiking patterns.
3. These stable spiking patterns are in sharp contrast to the chaotic response that exists for strong inhibition on an open set of nonzero Lebesgue measure in the parameter space.
4. Using the universality principles of the circle-map class, we are able to prove that our experimental observations are not dependent on specific preparations of the system but are “generic” results.

For natural neocortical neural networks, we propose that the above-described responses play a role similar to the unstable periodic orbits in chaotic dynamical systems (Grebogi et al. 1988; Ott et al. 1990). There, the periodic orbits provide a firm backbone for the complex structure that is hidden in the seemingly intractable chaotic activity. This view justifies an even closer examination of the local firing behavior.

3 Efficient Arnol'd coding

The activity of a perturbed neuron naturally defines a dynamical system. An *encoding* of a dynamical system consists of a partition of a usually continuous phase-space of the evolving system into areas that then are symbolically labeled, for example, by letters. Each time the system's trajectory enters a specific area of the phase-space, the associated letter is reported. The code is useful if it succeeds in the discrimination of states in an unambiguous way, up to a chosen precision, by a symbol sequence of sufficient length. Let us reconsider a neural network that consists of a number of coupled noise-driven limit-cycles. Intrinsically, the Arnol'd tongue structure provides a local coding scheme of the network evolution, where noise levels and neuron excitabilities, which fully describe the local states, are encoded by the periodicity of the spiking of the targeted neurons and by their spiking frequencies. This coding process can be schematically expressed in the following form:

$$\text{Coding: } \{f_1, f_2\} \rightarrow \{p, (f'_2)\} , \quad (4)$$

where f_1 is the frequency of the perturbing neuron, f_2 is the intrinsic frequency of the perturbed neuron, f'_2 is the frequency of the perturbed neuron (bracketed since it generally differs only little from f_2), and p labels the

periodicity. When the local network state changes in time, this corresponds to a trajectory in the $\{\Omega, K\}$ -space. Along the trajectory, various periodic spiking patterns are emitted. They constitute an encoding of the trajectory. Figure 4 indicates what the encoding sequence looks like when Ω is slowly increased (e.g. due to slow local gradients of the noisy input), at fixed interaction strength $K = 1$. Let us focus on some special properties of this code. Indeed, it is a code that is

1. *robust against adaptation and relaxation processes* [the experimental relaxations towards the asymptotic solutions are very fast, of the order of one interspike interval, for periods < 10 (Stoop et al. 2000a)],
2. *independent of the level of excitation in a homogeneously excited area* [$\Omega = T_s/T_o$ is able to respond to local gradients of the noise level but remains fixed under homogeneous changes of the network activity],
3. *has optimal coding properties, similar to the Huffman code* (Huffman 1952; Ash 1965) [the shortest code (period 1) corresponds to the largest partition element in the parameter-space, the second shortest (period 2) to the second largest, etc. For signals that are equidistributed on the $\{\Omega, K\}$ -parameter space, this coding is therefore optimally efficient],
4. *self-refining under increased network activity* [in vitro experiments with neocortical pyramidal neurons, we found that for low activity in relation to the speed of parameter change, only the lowest periodicities (1, 2, 3, 4, ...) are returned. To return longer, more complex periodicities, higher spiking frequencies must be used. In this way, increased spiking activity leads to a hierarchical refining of the low-activity encoded signal], and
5. *able to represent spike-time coding as well as frequency-coding* [frequency-encoded network-input essentially modifies Ω , whereas spike-time coded input essentially leads to an increase in K . In this way, both presently discussed coding schemes are naturally embedded in the Arnol'd code].

4 Phase-coincidence and synchronization

To arrive at a network that can perform neocortical perception tasks, the interaction between the strongly coupled subsystems must be defined. To this end, and to include medium-size interaction, we refine our model of cortical activity by using a coupled-map lattice approach with diffusive coupling (Bunimovich and Sinai 1988; Losson and Mackey 1994). On this level of description, the binary interaction maps are assumed to act on equal time scales. In spite of the increased level of abstraction, this refined model still incorporates the generic properties of noise-driven networks. The site maps in this coupled-map lattice consist of randomly excitatory/inhibitory binary interaction maps $f_{\Omega K}$, where also Ω and K are chosen at random. In the numerical experiments below, the local excitabilities K (cf. Eq. 2) were taken from the interval $[0.3, 0.8]$, monitoring in this way rather massive coherent packages of transmitted infor-

mation. The diffusive coupling is established by the update-rule

$$\phi\{i, j\}(t_{n+1}) := (1 - k_2 k\{i, j\}) f_{K\Omega}(\phi\{i, j\}(t_n)) + k_2 / nm \sum_{nn} k\{i, j\} \phi\{k, l\}(t_n), \quad (5)$$

where ϕ is the phase of the phase-return map at the indexed site, and nm again denotes the cardinality of the set of all next-neighbors of site $\{i, j\}$. The overall coupling among the site maps is described by k_2 . This global coupling strength is locally modified by realizations $k\{i, j\}$ taken from some distribution, which may or may not have a first moment (in the first case, k_2 can be normalized to be the global average over the local coupling strengths). In (5), the first term reflects the degree of self-determination of the phase at site $\{i, j\}$; the second term reflects the influence by next-neighbors, which are again understood in the sense of strongest interaction. A moderate example of the spatio-temporal behavior of this network is shown in Fig. 6.

For biologically reasonable parameters, the response of the network is essentially unsynchronized, in spite of the coupling. Extrapolations from simpler models, for which exact results are available (Bunimovich and Sinai 1988; Losson and Mackey 1994), provide us with the reasons why. Generically, from weakly coupled regular systems, regular behavior can be expected. If only two systems are coupled, generally a simpler period than the

maximum of the involved periodicities emerges. If, however, more partners are involved, a competition sets in, and high periodicities most often are the result. Typically, synchronized chaotic behavior results from coupling chaotic and regular systems, if the chaotic contribution is strong enough. Otherwise, the response will be regular. When chaotic systems are coupled, however, synchronized chaotic behavior as well as macroscopically synchronized regular behavior may be the result (Bunimovich and Sinai 1988; Losson and Mackey 1994). For obtaining fully synchronized networks, the last possibility is of special interest.

Figure 7a illustrates these findings for a model of coupled *identical* tent maps [where the results have been obtained analytically following Losson and Mackey (1994) and by using thermodynamic formalism methods]. In Fig. 7b we demonstrate the good correspondence between this model and the more general network that we are interested in. As a function of the slope a of the local tent map (which corresponds to the local excitability K) and of the coupling strength k_2 , contour lines indicate the instability of the network patterns. As can be seen, due to the coupling, even for locally chaotic maps ($a > 1$), stable network patterns may evolve (often in the form of statistical cycling; see Losson and Mackey 1994). Upon further increasing the local instability, finally chaotic network behavior emerges. Unfortunately, in the case of measured neuronal phase return maps, this possibility only exists for the inhibitory connections.

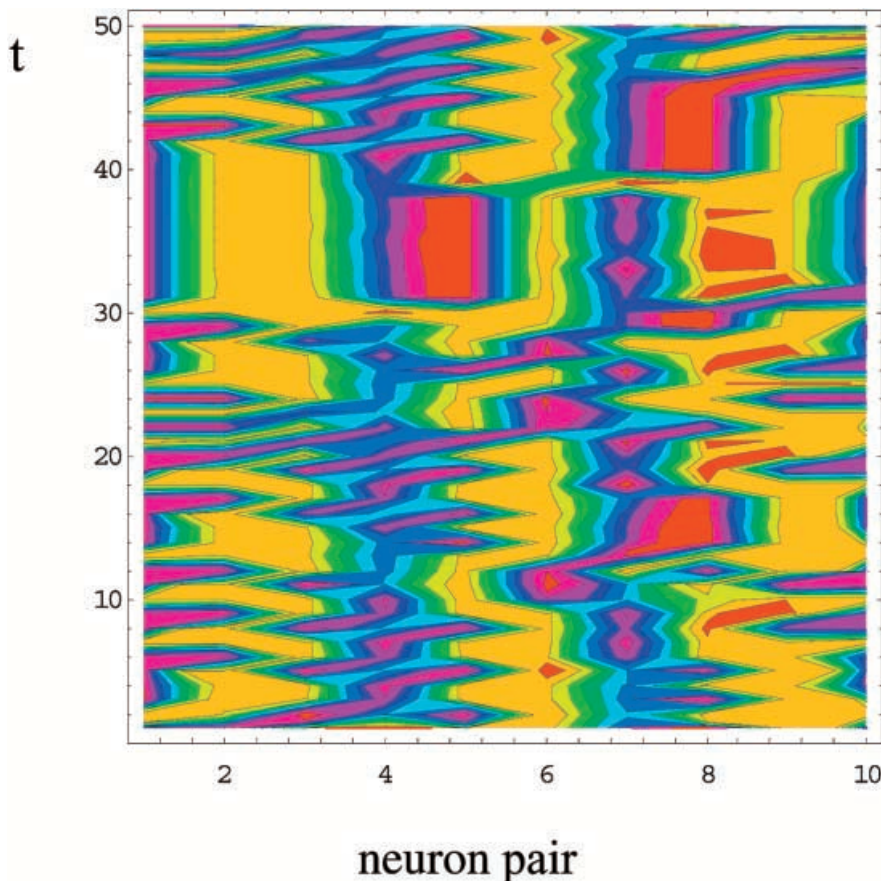


Fig. 6. Complex spiking behavior from the phase-coupled model. Time development of a chain of $n = 10$ diffusively coupled binary interaction maps, of inhibitory and of excitatory type, where the phases are distinguished by colors

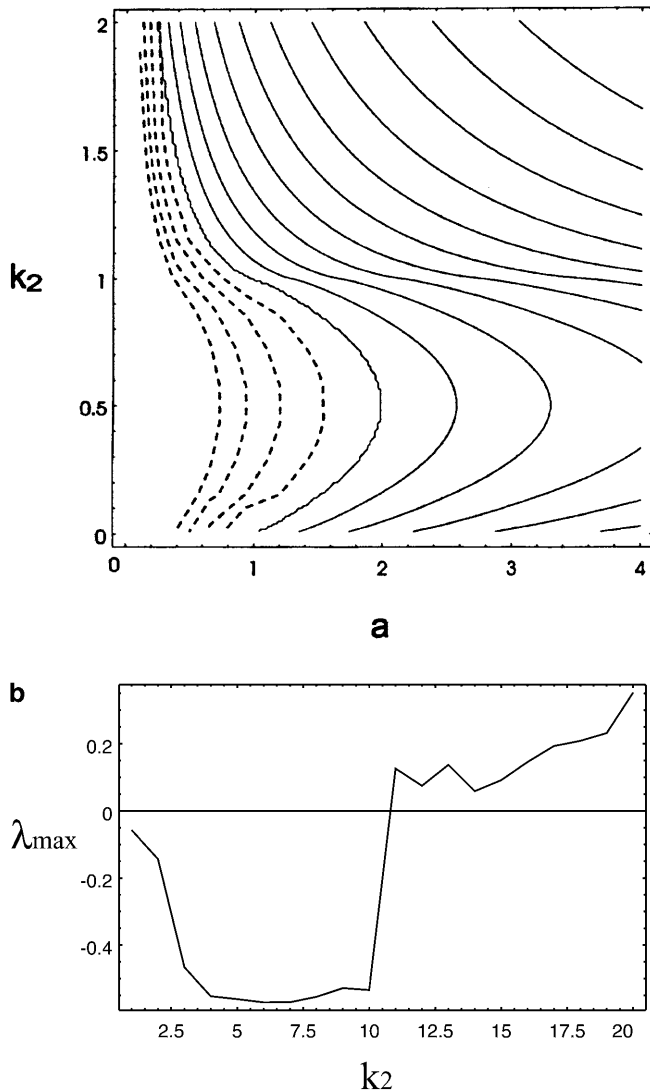


Fig. 7. **a** Network Lyapunov exponent λ_n describing stability of patterns of a network of coupled tent maps, as a function of the (identical) site maps slopes a and coupling k_2 . Contour lines of distance 0.25 are drawn *dashed* where stable network patterns evolve ($\lambda_n < 0$), starting with $\lambda_n = -1$ (leftmost curve). **b** Maximal site-Lyapunov exponent λ_{\max} of a network of locked inhibitory site maps, as a function of the coupling k_2 . For the network, the local excitability is $K = 0.5$ for all sites and Ω is from the interval $[0.8, 0.85]$. The behavior of this network closely follows the behavior predicted by the tent-map model

Furthermore, the part of the parameter space on which the maps would need to dwell is rather small (although of nonzero measure). Therefore, additional fine tuning (e.g. by thalamic “control” circuits) may be necessary for putting a large number of inhibitory connections into synchronizing working conditions. The latter conditions have been postulated as necessary for the performance of perception tasks (Singer 1994; Von der Malsburg 1994).

5 Phase-coincidence learning

As an alternative to control mechanisms, we tested *phase-coincidence-based Hebbian learning* schemes

[which modify the connection strengths between the lattice sites (Hebb 1949; Abeles 1982; Koch 1999)]. To explore this possibility, we use a hyperbolic tangent function to discriminate between phase-coincident neighboring site maps (whose connection strengths will be enhanced) and out-of-phase neighboring site maps (whose connection strengths will be reduced). The update rule for the connection strengths is

$$k\{i, j\}(t_{n+1}) := k\{i, j\}(t_n)(\text{Tanh}[r] + 1)/2, \quad (6)$$

where r is the sum of the absolute inverse differences Δ_ϕ between the phase at the lattice point against the phases of its neighbors. A biophysically reasonable cutoff (e.g. $\Delta_\phi < 0.01$ to $\Delta_\phi = 0.01$) prevents divergent influence of nearly equally phased neighbors. The immediate effect of the update rule is to suppress the connection k only at strongly out-of-phase sites. For the large majority of sites with in-phase connections, the rule is without a noticeable effect. The involved (small) decrease of the total sum of connection strengths can be compensated by a corresponding factor, or the decrease can be interpreted as an adaptation effect that is balanced when the input pattern is changed (see below). The biological idea behind this implementation is that network elements taking part in a specific perception task will be synchronized, whereas the remaining elements will be disconnected from this process. Under this Hebbian phase-coincidence learning, the connection strengths $k\{i, j\}$ converge within a few (< 10) iterations to (for practical purposes) fixed values. To investigate the pattern discrimination properties of this network, we chose one horizontal layer of a two-dimensional network to be the input layer. On this layer, we implemented distinct phase profiles, to model different sensory inputs. A comparison of the emerging network patterns, as a function of the inputs, yields the following results. As a function of the inputs, only a small number of localized, input-specific *coding sites* modify their phases (see Fig. 8a). To obtain this figure, the phase differences evoked by two distinct sensory inputs were plotted, using color coding. The large red sea represents the part of the network where no significant phase changes are induced. Within this sea, the coding sites emerge as small islands (note that the phase differences in the bottom layer reflect the distinct input signals and that the top layer is affected through the cyclic boundary conditions). In this way, input information is directly transferred to specialized network sites, from where it may be read off and processed. From the simulations, two remarkable properties emerge. Similar input patterns generate similar coding-site patterns (quite in the sense of a metric), and coding-site activities generally are of a periodic nature. The latter property is demonstrated in Fig. 8b, where inputs from three patterns are compared. Figure 8c shows how large excitatory refractory periods strongly enhance synchronization. In contrast, strong local inhibitory circuits enhance the formation of isolated coding sites, whose preferred location seems to be at boundaries between inhibitory and excitatory interactions.

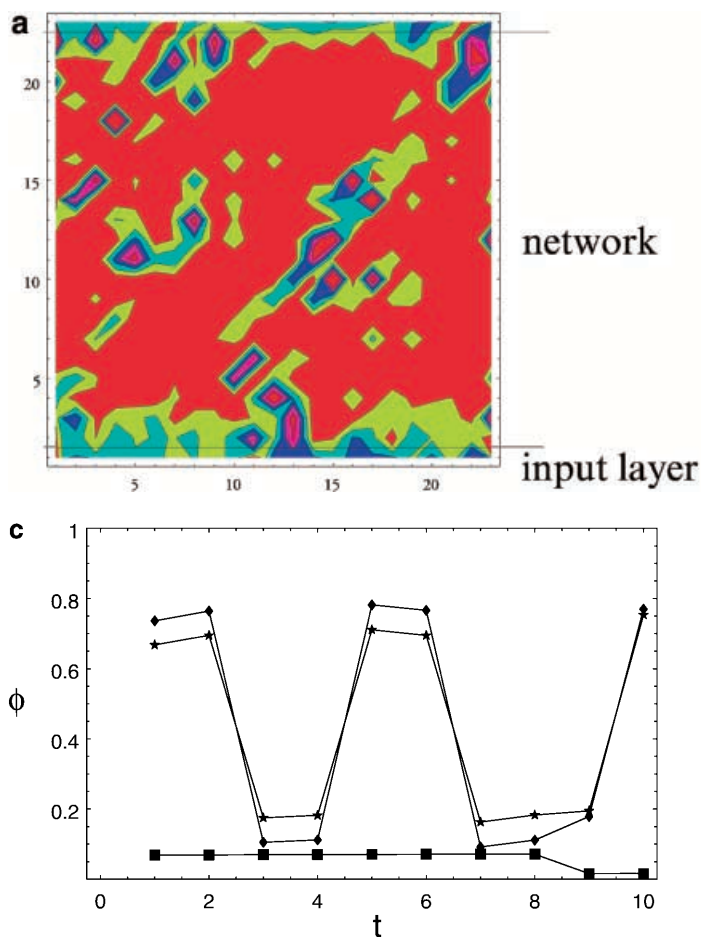


Fig. 8. **a** Phase differences evoked by two distinct input patterns (2-d network, evolution under phase-coincidence detection). In the *red area*, no changes are observed. The *bottom layer* (= input layer) shows the differences in the input patterns. Due to two-torus periodic boundary conditions, this also affects the top layer. Coding sites are the islands within the red sea. At these sites, prominent phase changes are observed. **b** Corresponding figure when excitatory phase return maps have extended refractory periods. A visibly increased “penetration depth” of coding sites indicates increased degree of synchronization. **c** Temporal phase difference evolution, at a coding site from (a). Three input signals were compared (constant random phase layer l_1 , constant layer l_2 with phase 0.2, constant layer l_3 with phase 0.6). Absolute phase differences are shown of, *top curve*: $l_1 - l_2$, *medium curve*: $l_1 - l_3$, *bottom curve*: $l_2 - l_3$

These findings may be relevant to perception and feature binding. The feature-binding problem relates to the cortical task of associating one single object with its different features (Singer 1994, Von der Malsburg 1994). In the context of our approach, it is natural to identify subsets of coding site activity with the representations of different object features. Correspondingly, the set of temporally varying coding sites could be interpreted as a spatio-temporal object representation, or, at least, a pre-state thereof. For this interpretation to make sense, the metric property mentioned above is of importance. Moreover, also the amount of time needed for the convergence of coding sites is in the range typically needed for perception tasks (a few 100 ms).

6 Conclusions

From our combined experimental, theoretical, and numerical studies, we draw the following conclusions:

1. Arnol'd tongues may provide an efficient coding scheme for cortical activity. This coding unifies frequency coding with spike-time coding. The code is optimal in an information-theoretic sense.
2. Locally, chaotic response emerges on a nonzero measure of the parameter space accessible only to strong inhibitory perturbations. This implies that in

the brain, chaotic behavior is already introduced on a local level. On the global level, complex behavior emerges from the competition between different stable n -ary interactions (where $n = 2, 3, \dots$). This competition is mediated by medium-size synaptic inputs, which in our model are represented by phase coupling.

3. Possible local chaotic behavior does not desynchronize but rather may contribute to a synchronization of the network. Synchronization is impossible for the quasi-static phase-coupled networks at moderate local coupling, unless strong inhibitory circuits are active (strong inhibitory circuits correspond to the modeling case $k_2 = 1$). In the latter case, the synchronization effect is largely independent from the local coupling strengths K . Detailed simulations show that synchronization is enhanced by large refractory periods (Stoop et al. 1999).

To what extent finally the brain makes use of these principles can only be speculated at the moment. Refined investigations are needed to answer this issue more profoundly. From the point of view of computation, it is obvious that the proposed encoding in terms of periodicities would be very efficient (in comparison with binary elements with no optimized coding), especially if the self-refining property of the coding is taken into account. In future, we need to study this concept in more

detail to see whether it can prove useful for the design of computationally more powerful hard- and software.

Acknowledgements. This work was supported by the SNSF and Phonak AG (KTI-contract). The authors acknowledge discussions with R.J. Douglas and Y.G. Sinai.

References

- Abeles M (1982) Local cortical circuits. Springer, Berlin Heidelberg New York
- Argyris J, Faust G, Haase M (1994) Exploration of chaos. North-Holland, Amsterdam
- Ash RB (1965) Information theory. Dover, London
- Baesens C, Guckenheimer J, Kim S, MacKay RS (1991) Three coupled oscillators: mode-locking, global bifurcations and toroidal chaos. *Physica D* 49: 387–475
- Bunimovich LA, Sinai YG (1988) Space-time chaos in coupled map lattices. *Nonlinearity* 1: 491–516
- Chillemi S, Barbi M (eds) (1999) Chaos and noise in biology. World Scientific, Singapore
- Cornfeld EP, Fomin SV, Sinai YG (1982) Ergodic theory. Springer, Berlin Heidelberg New York
- Feller W (1971) An introduction to probability theory and its applications, vol 2. Wiley, New York
- Glass L, Mackey M (1988) From clocks to chaos. Princeton University Press: Princeton, N.J.
- Glass L, Guevara M, Belair J, Shrier A (1984) Global bifurcations of a periodically forced biological oscillator. *Phys Rev A* 29: 1348–1357
- Grebogi C, Ott E, Yorke JA (1988) Unstable periodic orbits and the dimensions of multifractal chaotic attractors. *Phys Rev A* 37: 1711–1715
- Hebb D (1949) The organization of behavior. Wiley, New York
- Hines M (1989) A program for simulation of nerve equations with branching geometries. *Int J Biomed Comput* 24: 55–68
- Hines M (1994) The neuron simulation program. In: Skrzypek J (ed) Neural network simulation environments. Kluwer, Amsterdam, pp 147–163
- Huffman DA (1952) A method for the construction of minimum-redundancy codes. *Proc IRE* 40: 1089–1101
- Koch C (1999) Biophysics of computation. Oxford University Press, Oxford
- Losson J, Mackey M (1994) Coupling-induced statistical cycling in two diffusively coupled maps. *Phys Rev E* 50: 843–856
- Ott E, Grebogi C, Yorke JA (1990) Controlling chaos. *Phys Rev Lett* 64: 1196–1199
- Peinke J, Parisi J, Roessler OE, Stoop R (1992) Encounter with chaos. Springer, Berlin Heidelberg New York
- Reyes AD, Fetz EE (1993) Two modes of interspike interval shortening by brief transient depolarizations in cat neocortical neurons. *J Neurophysiol* 69: 1661–1672
- Schindler K, Bernasconi C, Stoop R, Goodman P, Douglas RJ (1997) Chaotic spike patterns evoked by periodic inhibition of rat cortical neurons. *Z Naturforsch* 52a: 509–512
- Singer W (1994) Putative functions of temporal correlations in neocortical processing. In: Koch C, Davis J (eds) Large-scale neuronal theories of the brain. MIT Press/Bradford Books, Cambridge, Mass., pp 201–237
- Stoop R, Steeb W-H (1997) Chaotic family with smooth Lyapunov dependence. *Phys Rev E* 55: 7763–7766
- Stoop R, Schindler K, Bunimovich LA (1999) Inhibitory connections enhance pattern recurrence in networks of neocortical pyramidal cells. *Phys Lett A* 258: 115–122
- Stoop R, Schindler K, Bunimovich LA (2000a) When pyramidal neurons lock, when they respond chaotically, and when they like to synchronize. *Neurosci Res* 36: 81–91
- Stoop R, Schindler K, Bunimovich LA (2000b) Noise-driven neocortical interaction: complex neuron spiking uncovered by nonlinear dynamics. *Acta Biotheor* 48: 149–171
- Von der Malsburg C (1994) The correlation theory of brain function. In: Domany E, van Hemmen J, Schulten K (eds) Models of neural networks II. Springer, Berlin Heidelberg New York, pp 95–119